HHS Public Access

Author manuscript

Alzheimer Dis Assoc Disord. Author manuscript; available in PMC 2018 January 01.

Published in final edited form as:

Alzheimer Dis Assoc Disord. 2017 ; 31(1): 1–7. doi:10.1097/WAD.0000000000000188.

Fluorodeoxyglucose Positron Emission Tomography (FDG-PET) Correlation of Histopathology and MRI in Prion Disease

Karin P. Mente, MD, MS[1,2], **James K. O'Donnell, MD**[3], **Stephen E. Jones, MD, PhD**[4], **Mark L. Cohen, MD**[5,6], **Nicolas R. Thompson, MS**[7], **Alberto Bizzi, MD**[8], **Pierluigi Gambetti, MD**[5,6], **Jiri G. Safar, MD, PhD**[5,6,9], and **Brian S. Appleby, MD**[5,6,9]

[1]Neurology, Cleveland Clinic, Cleveland, Ohio, USA

[3]Radiology, University Hospitals Case Medical Center, Cleveland, Ohio, USA

[4]Diagnostic Radiology, Cleveland Clinic, Cleveland, Ohio, USA

[5]Pathology, University Hospitals Case Medical Center, Cleveland, Ohio, USA

[6]National Prion Disease Pathology Surveillance Center, Cleveland, Ohio, USA

[7]Quantitative Health Sciences, Cleveland Clinic, Cleveland, Ohio, USA

[8]Neuroradiology, Humanitas Research Hospital IRCCS, Milano, Italy

[9]Neurology, University Hospitals Case Medical Center, Cleveland, Ohio, USA

Abstract

Creutzfeldt-Jakob disease (CJD) and other prion diseases are rapidly progressive spongiform encephalopathies that are invariably fatal. Clinical features and MRI, EEG, and CSF abnormalities may suggest prion disease, but a definitive diagnosis can only be made by means of neuropathological examination. Fluorodeoxyglucose positron emission tomography (FDG-PET) is not routinely used to evaluate patients with suspected prion disease. This study includes 11 cases of definite prion disease in which FDG-PET scans were obtained. There were 8 sporadic CJD cases, 2 genetic CJD cases, and 1 fatal familial insomnia case. Automated FDG-PET analysis revealed parietal region hypometabolism in all cases. Surprisingly, limbic and mesolimbic hypermetabolism were also present in the majority of cases. When FDG-PET hypometabolism was compared with neuropathological changes (neuronal loss, astrocytosis, spongiosis), hypometabolism was predictive of neuropathology in 80.6% of cortical regions versus 17.6% of subcortical regions. The odds of neuropathologic changes were 2.1 times higher in cortical regions than subcortical regions (p=0.0265). A similar discordance between cortical and subcortical regions was observed between FDG-PET hypometabolism and MRI DWI hyperintensity. This study shows that there may be a relationship between FDG-PET hypometabolism and neuropathology in cortical regions in prion disease but it is unlikely to be helpful for diagnosis.

Correspondence to: Karin Mente, NIH/NINDS, 10 Center Drive, Bethesda, MD 20892; Telephone: (301) 402-3596; Fax: (301) 480-2286; Karinmentemd@gmail.com.

[2]Present Address: National Institute of Neurological Disorders and Stroke, National Institutes of Health, Bethesda, Maryland, USA

Keywords

prion diseases; CJD; positron emission tomography; MRI; neuropathology

Introduction

Creutzfeldt-Jakob disease (CJD) is a rapidly progressive transmissible spongiform encephalopathy, also known as prion disease. Other prion diseases include fatal familial insomnia (FFI), Gerstmann-Sträussler-Scheinker disease, and kuru. Individuals afflicted by prionopathies have a short symptomatic period that rapidly progresses to death over several months. Definitive diagnosis requires neuropathological evaluation of brain tissue, usually in the form of an autopsy[1].

The clinical presentation of prionopathies is variable. In CJD, patients develop a rapidly progressive dementia along with cerebellar ataxia, vision deficits, myoclonus, and/or pyramidal or extrapyramidal signs and symptoms that often culminates in akinetic mutism[2]. In contrast to CJD, individuals with FFI have prominent sleep disturbances, weight loss, autonomic instability, voice changes, cognitive deficits, ataxia, visual disturbances, and myoclonus[3].

CJD is the most common human prion disease. It exists in sporadic, genetic, and acquired forms. Sporadic CJD is the most common form with an annual incidence of about 1 case per 1 million persons[4]. The etiology of sporadic CJD is unclear, but it has been suggested that a post-translational modification may play a role in prion protein misfolding or other conditions, such as aging, may allow abnormal prion proteins to stabilize and accumulate[5]. Sporadic CJD is classified according to its molecular subtype. There are seven molecular subtypes, MM1, MM2-C, MM2-T, MV1, MV2, VV1, and VV2 that are based on the polymorphism at codon 129 of the prion protein gene (*PRNP*) and the prion protein type. Each molecular subtype is associated with a specific clinical phenotype and pattern of neuropathological changes[6]. Genetic CJD is classified according to mutations in *PRNP*, the most common mutation of which is E200K[7]. Like sporadic CJD, genetic CJD also shows phenotypic variability[8]. Phenotypic heterogeneity also occurs in acquired CJD, a category which includes variant CJD, which is linked with bovine spongiform encephalopathy, and cases of iatrogenic transmission[9].

In spite of the variable clinical presentations in prionopathies, the diagnostic evaluation in any patient suspected of having a prionopathy includes brain MRI, EEG, and CSF analysis[10]. MRI patterns suggestive of CJD are FLAIR or DWI hyperintensity in temporal, parietal, or occipital cortex and/or the caudate and putamen, but restricted diffusion on DWI sequence with correlation on apparent diffusion coefficient images is more specific for CJD than FLAIR hyperintensity[2,11]. On EEG, periodic sharp wave complexes have been reported in 64% of CJD cases[12]. In CSF, 14-3-3 and tau levels are positive in 88% to 91% and 81% to 90% of CJD cases, respectively, depending on timing of the lumbar puncture, but patients with other neurological disorders, such as stroke, other neurodegenerative diseases, and encephalitis, may have false positive 14-3-3 and tau levels[13–15]. Recently, an ultra-sensitive

assay called real time quaking induced conversion (RT-QuIC) enables detection of abnormal prion protein seeding in cerebrospinal fluid of patients affected by prion disease[16].

Other imaging modalities, such as positron emission tomography (PET) have been studied in CJD although there are few studies with autopsy-confirmed cases of prion disease. One study in 2002 with fluorodeoxyglucose (FDG) as a tracer found hypometabolism primarily in the parietal region[17]. Another study with FDG also found hypometabolism in the temporal and parietal regions, and the cerebellum[18]. However, each of these studies involved only 5 definite CJD cases. Another study including one definite, seven probable, and three cases of possible sCJD demonstrated extensive cortical hypometabolism without involvement of the basal ganglia or thalamus[19]. One paper was able to correlate FDG-PET findings with neuropathologic findings in a single case of CJD[20]. Currently, PET imaging is not routinely used in the diagnostic evaluation of prion disease patients. In this retrospective study, we compare FDG-PET metabolic patterns with brain MRI findings and neuropathological changes in cases of definite prion disease in an effort to further understand neuroimaging correlates of neuropathological changes in prion diseases.

Methods

Subjects

The Cleveland Clinic electronic medical record system was queried for cases of prion disease from 2003 to 2013 using the International Classification of Disease (ICD-9) codes for prion diseases, 046.**. This search resulted in 23 cases fulfilling criteria for probable or possible CJD from Zerr *et al*[2]. 11 of the 23 cases had brain FDG-PET and brain autopsy so these cases were included in this study. There were 8 definite neuropathology-confirmed sporadic CJD cases, 2 definite genetic CJD cases, and 1 definite case of FFI. The mean age at disease onset was 59.8 ± 3.3 years with an age range of 39 to 79 years. There were 5 males and 6 females. There was no family history of prion disease or rapidly progressive dementia in any patients, including patients with genetic CJD and FFI.

The PET scans were performed at Cleveland Clinic in 7 of the 11 subjects in a PET/CT scanner, Biograph mCT (Siemens, Munich, Germany). In the remaining 4 subjects, PET scans were performed at community facilities and images were obtained for review. Brain CT at the time of FDG-PET was used for attenuation correction. Blood glucose range at the time of FDG injection was 96 to 141 mg/dl. Images were acquired about one hour after FDG injection. None of the patients were under sedation or anesthesia. The patients did not have seizures around the time of the PET scan. One neuroradiologist and one nuclear medicine physician independently interpreted FDG-PET images visually.

Brain MRI was performed within one month of PET scanning. Two neuroradiologists reviewed DWI and FLAIR images independently.

The Institutional Review Boards at both Cleveland Clinic and University Hospitals Case Medical Center approved this study.

Automated PET Analysis

FDG-PET images were analyzed using MIM Neuro software (MIM, Cleveland, OH, USA). FDG-PET images were co-registered to brain MRI for anatomic segmentation based on a template. Then, FDG-PET was normalized to whole brain activity and compared against a normal database to determine presence of hypermetabolism and hypometabolism on the basis of standardized uptake values (SUV). The MIM normal database consists of brain FDG-PET scans from 43 male and female subjects with mean age 63 ± 10 years and age range of 41 to 80 years. Subjects did not have histories of primary brain neoplasms, brain metastases, head/neck radiation, chemotherapy, medications that could affect cerebral glucose metabolism, head trauma, stroke, substance abuse, leukemia, renal failure, severe heart failure, severe chronic obstructive pulmonary disease, uncontrolled diabetes, or immune suppression. All volunteers in the normal control group had Mini Mental Status Exam (MMSE) scores of 25 or higher and Memory Impairment Screen (MIS) scores of 6 or higher.

Regional SUV was converted to z-scores for defining FDG metabolism. FDG-PET hypometabolism was defined as a z-score of less than −1.65, and hypermetabolism was defined as z-score of greater than 1.65 for $p < 0.05$.

Neuropathology

Brain autopsy was performed at the National Prion Disease Pathology Surveillance Center after consent for autopsy and research was obtained from patients' next of kin. Postmortem interval was less than 24 hours. Hematoxylin and eosin staining on fixed sections of brain tissue from frontal, temporal, parietal, and occipital cortices, cingulate gyrus, basal ganglia, thalamus, midbrain, brainstem, and cerebellum of one hemisphere were obtained for analysis of neuronal loss, reactive astrocytosis, and spongiosis. Western blot of unfixed brain homogenate was performed after proteinase K digestion with 3F4 monoclonal antibody (from Dr. Richard Kascsak, New York Institute for Basic Research), which binds to PrP^{Sc}. Immunohistochemistry was performed with monoclonal antibody 3F4 based on the method in Parchi *et al*[6]. Immunohistochemistry for glial fibrillary acidic protein (GFAP) was performed using an anti-GFAP monoclonal antibody (Sigma, St. Louis, MO, USA).

Genetic Analysis

Genomic DNA was extracted from unfixed frozen brain tissue. The *PRNP* gene was amplified with polymerase chain reaction and analyzed as previously described[6].

Statistical Analysis

Statistical analyses were performed using SPSS version 21 (IBM Corp., Armonk, NY, USA) for descriptive statistics with means +/− SE and R version 3.1.1 (R Core Team) was used for mixed effects logistic regression model. P-values less than 0.05 were considered statistically significant.

In the mixed effects logistic regression model, neuropathological findings of neuronal loss, astrocytosis and spongiosis and FDG-PET hypometabolism from automated PET analysis of the same hemisphere were compared. Neuronal loss, astrocytosis, and spongiosis were

compared together, similar to Parchi *et al*[6]. For each cortical and subcortical structure and region, we computed the proportion and percentage of cases where FDG-PET indicated absence of hypometabolism and when histopathology indicated absence of neuronal loss, astrocytosis, or spongiosis. Cortical regions include frontal, temporal, parietal, and occipital cortices. Subcortical regions include basal ganglia, hippocampus, thalamus, midbrain, brainstem, and cerebellum. Similarly, we computed the proportion and percentage for each area of FDG-PET hypometabolism when there was presence of neuronal loss, astrocytosis, and/or spongiosis. To determine whether hypometabolism was associated with neuronal loss, astrocytosis, and spongiosis on hematoxylin-eosin staining, we created a mixed-effects logistic regression model. The dependent variable was the presence or absence of neuronal loss, astrocytosis, and spongiosis on autopsy and the predictor was the presence or absence of hypometabolism on FDG-PET, treated as a fixed effect. We included brain region (cortical versus subcortical structures) as a covariate, also treated as a fixed effect. To account for correlated responses within a patient, we included a random effect for each patient. We computed the odds ratio and a 95% confidence interval for the effect of presence or absence of hypometabolism on presence or absence of neuronal loss/astrocytosis/spongiosis. Similarly, a mixed effects logistic regression model was used to determine the percentage of DWI hyperintensity in regions where there was hypometabolism on FDG-PET.

Results

Patient Characteristics

A total of 11 patients are included in this case series (see Table 1). All patients presented with dementia. Other signs and symptoms related to prion disease include visual deficits, pyramidal signs of weakness or hyperreflexia, extrapyramidal signs of cogwheel rigidity, decreased arm swing, and decreased stride length, or dystonia, cerebellar ataxia, myoclonus, insomnia, and behavior changes, including agitation and anxiety. Mean survival was 11.7 ± 2.6 months. Mean onset to PET scan was 5.9 ± 1.1 months. 6 patients had PET scans within the first half of their illness. CSF 14-3-3 protein was positive in 4 cases. CSF tau was positive in 5 cases. Both 14-3-3 and tau were positive in 4 cases. RT-QuIC results are not available as these cases were collected before RT-QuIC was routinely performed on CSF samples in the United States. Brain MRI showed cortical and/or caudate restricted diffusion in 9 cases. Among the sporadic CJD cases, there were 2 cases each of MM1, MM2-C, MV2, and VV2 molecular subtypes.

Automated PET Analysis

Attention was turned to automated PET analysis. FDG-PET hypometabolism was found in a few regions, most frequently in the posterior cingulate gyrus and precuneus, both of which are in the parietal lobe. Surprisingly, hypermetabolism was identified in the limbic and mesolimbic structures, including insula, medial temporal lobe, nucleus accumbens, olfactory cortex, and parahippocampal gyrus. The most frequently encountered hypometabolic and hypermetabolic regions, based on anatomic segmentation from a template, are listed in Table 2.

Comparison of FDG-PET and Neuropathology

The mixed effects logistic regression model was used to compare FDG-PET hypometabolism and the neuropathological findings of neuronal loss, astrocytosis, and spongiosis. Typical FDG-PET and neuropathological changes in CJD are highlighted in Figure 1.

Among all prion disease cases, there were a total of 36 cortical regions with neuronal loss, astrocytosis and/or spongiosis, and in FDG-PET, there were a total of 29 cortical regions (80.6%) with hypometabolism. Conversely, of the 34 subcortical regions where neuropathology revealed neuronal loss, astrocytosis and/or spongiosis, only 6 regions (17.6%) had hypometabolism on PET (see Figure 2 and Table 3). Table 3 lists the percentage of regions across patients with neuronal loss, astrocytosis, and/or spongiosis, in which there was hypometabolism on FDG-PET. Data on regions without neuronal loss, astrocytosis, or spongiosis are included in Table 1 in Supplementary Data.

The mixed-effects logistic regression model revealed a positive but non-significant relationship between autopsy-identified neuronal loss/astrocytosis/spongiosis and FDG-PET hypometabolism (odds ratio 3.9, p-value = 0.1268, 95% confidence interval = 0.1 to 24.0). The model also revealed that the odds of neuronal loss/astrocytosis/spongiosis occurring with FDG-PET hypometabolism were 2.1 times higher in the cortical regions than subcortical regions (95% confidence interval 1.4 to 61.9, p-value=0.0265). There was no difference between PET scans from the first half of illness and second half of illness since onset. FDG-PET metabolism could not be compared with specific neuropathological changes within brain regions (e.g., astrocytosis, spongiosis, etc.) given the neuropathologic rating scale used, heterogeneity of staining amongst cases, and the small sample size.

Comparison of FDG-PET and MRI

FDG-PET hypometabolism and DWI hyperintensity were compared. In a mixed effects logistic regression model, 51.5% of cortical regions that were hypometabolic on FDG-PET were hyperintense on DWI. For subcortical regions, 28.6% of regions that were hypometabolic on FDG-PET were hyperintense on DWI. Please refer to Table 2 in Supplementary Data for further details on regional MRI DWI hyperintensity and PET hypometabolism comparisons.

Discussion

A pattern of parietal region hypometabolism, and limbic and mesolimbic system hypermetabolism was identified in brain FDG-PET scans of patients affected by prion disease in this study. There was a correspondence between FDG-PET hypometabolism in cortical regions (frontal, temporal, parietal, and occipital) and neuropathological changes with neuronal loss, reactive astrocytosis, and spongiosis in cortical regions.

The high frequency of parietal region FDG hypometabolism, as exemplified by precuneus hypometabolism in all cases of prion disease and posterior cingulate gyrus hypometabolism in 10 out of 11 cases in this study, is similar to previous reports of parietal region hypometabolism[17–20]. In studies of other neurodegenerative disorders, such as Alzheimer

disease and dementia with Lewy bodies, and in animal models of temporal lobe epilepsy, FDG-PET hypometabolism corresponds to neuronal loss[21–23]. Hence, FDG-PET hypometabolism is consistent with neuropathologic lesion patterns observed in prion disease. Unfortunately, this pattern is also observed in other forms of dementia, most notably Alzheimer's disease.

Nevertheless, hypermetabolism in limbic and mesolimbic structures in FDG-PET has never been reported in prion disease and the source of FDG hypermetabolism is unclear. Hypermetabolism could be related to microglial activation, as has been suggested in cases of FDG-PET hypermetabolism in another neurodegenerative disease, amyotrophic lateral sclerosis, and in an animal study of ischemic stroke using FDG-PET where hypermetabolism corresponds to an area with activated microglia[24,25]. There is also evidence for microglial activation and neuroinflammation with increased expression of microglial markers in CJD[26–28]. In addition, Llorens *et al.* has found that there is regional variation in microglia activation depending on molecular subtype in sporadic CJD[29]. An alternative explanation for limbic and mesolimbic hypermetabolism was considered because hypermetabolism has been reported in other neurological disorders, such as limbic encephalitis[30]. Comorbid limbic encephalitis is unlikely in this study population because only one out of nine patients with testing for paraneoplastic antibodies was positive for a low titer anti-VGKC antibody in serum; this patient did not respond to immunomodulatory treatment. Furthermore, none of the patients had any neuropathologic evidence of encephalitis. This finding requires duplication and more detailed neuropathological examination in order to truly understand any potential significance.

This study provides support for a connection between FDG-PET hypometabolism and neuropathology in prion disease in cortical regions. When FDG-PET hypometabolism is compared with neuronal loss, astrocytosis, and spongiosis in histopathology, there is 80.6% agreement between hypometabolism and neuronal loss/astrocytosis/spongiosis in cortical regions. However, there is less agreement between FDG-PET hypometabolism and neuropathology for subcortical structures, including basal ganglia, hippocampus, thalamus, midbrain, brainstem, and cerebellum. However, we were unable to assess whether the relationship between FDG-PET hypometabolism and neuronal loss/astrocytosis/spongiosis was dependent on cortical versus subcortical regions in our mixed-effects model due to small sample size. Similar findings were observed in the study by Kim et al., which postulated a lack of relationship between spongiosis or prion protein deposition and FDG-PET hypometabolism[19]. Furthermore, in many subcortical regions, especially those in limbic and mesolimbic systems, there was FDG-PET hypermetabolism rather than hypometabolism. The presence of hypermetabolism could be related to microglial activation, and there is some evidence for microglial activation in CJD.

FDG-PET was also compared with MRI. Many regions with hypometabolism on PET did not show restricted diffusion on DWI. This discordance could be analogous to the situation in ischemic stroke imaging in which FDG-PET is more sensitive to ischemic changes than MRI[31]. Similar to our comparisons of FDG-PET hypometabolism with neuropathological changes, there was also less of a correlation between FDG-PET hypometabolism with restricted diffusion on MRI in subcortical as opposed to cortical regions.

Since this study is a retrospective case-series, there are limitations. First, the study population is very small because prion disease is uncommon. Because this was a retrospective study, PET scans were acquired in multiple PET scanners, which could potentially contribute to variability in detecting small differences in hypermetabolism and hypometabolism. With regard to neuropathology, there could be variability in detection of neuronal loss, astrocytosis, and spongiosis due to sampling error, in that tissue sections may not exactly correspond to anatomic segmentation in automated PET analysis. This study adds to the literature that brain FDG-PET scans have limited diagnostic utility in prion disease, especially when compared to brain MRI and CSF analyses. Despite limitations, FDG-PET could be considered a research tool in exploring pathology in prion disease in living patients, but further study is necessary to clarify the role of FDG-PET in diagnostic evaluations. A prospective study with more detailed neuropathological analyses is necessary to understand the relationship between FDG-PET metabolism patterns and neuropathology and could be helpful in further understanding the pathophysiology of prion diseases.

Supplementary Material

Refer to Web version on PubMed Central for supplementary material.

Acknowledgments

Funding

The National Prion Disease Pathology Surveillance Center is supported by the Centers for Disease Control and Prevention (grant UR8/CCU515004 to JGS).

The authors thank Dr. Richard Kascsak for the 3F4 antibody. The authors thank Ms. Katie Glisic for assistance. The authors also appreciate Dr. Ignazio Cali for review of immunohistochemistry in the E200K cases.

The normal FDG-PET image in Figure 1c is courtesy of MIM Software, Inc.

References

1. Puoti G, Bizzi A, Forloni G, Safar JG, Tagliavini F, Gambetti P. Sporadic human prion diseases: molecular insights and diagnosis. Lancet Neurol. 2012; 11:618–628. [PubMed: 22710755]
2. Zerr I, Kallenberg K, Summers DM, Romero C, Taratuto A, Heinemann U, Breithaupt M, Varges D, Meissner B, Ladogana A, Schuur M, Haik S, Collins SJ, Jansen GH, Stokin GB, Pimentel J, Hewer E, Collie D, Smith P, Roberts H, Brandel JP, van Duijn C, Pocchiari M, Begue C, Cras P, Will RG, Sanchez-Juan P. Updated clinical diagnostic criteria for Creutzfeldt-Jakob disease. Brain. 2009; 132:2659–2668. [PubMed: 19773352]
3. Krasnianski A, Sanchez Juan P, Ponto C, Bartl M, Heinemann U, Varges D, Schulz-Schaeffer WJ, Kretzschmar HA, Zerr I. A proposal of a new diagnostic pathway for fatal familial insomnia. J Neurol Neurosurg Psychiatry. 2014; 85:654–659. [PubMed: 24249784]
4. Holman RC, Belay ED, Christensen KY, Maddox RA, Minino AM, Folkema AM, Haberling DL, Hammett TA, Kochanek KD, Sejvar JJ, Schonberger LD. Human prion diseases in the United States. PLoS One. 2010; 5(1):e8521. [PubMed: 20049325]
5. Gambetti P, Cali I, Notari S, Kong Q, Zou WQ, Surewicz WK. Molecular biology and pathology of prion strains in sporadic human prion diseases. Acta Neuropathol. 2011; 121:79–90. [PubMed: 21058033]
6. Parchi P, Giese A, Capellari S, Brown P, Schulz-Schaeffer W, Windl O, Zerr I, Budka H, Kopp N, Piccardo P, Poser S, Rojiani A, Streichemberger N, Julien J, Vital C, Ghetti B, Gambetti P,

Kretzschmar H. Classification of sporadic Creutzfeldt-Jakob disease based on molecular and phenotypic analysis of 300 subjects. Ann Neurol. 1999; 46:224–233. [PubMed: 10443888]

7. Kovács GG, Puopolo M, Ladogana A, Pocchiari M, Budka H, van Duijn C, Collins SJ, Boyd A, Giulivi A, Coulthart M, Delasnerie-Laupretre N, Brandel JP, Zerr I, Kretzschmar HA, de Pedro-Cuesta J, Calero-Lara M, Glatzel M, Aguzzi A, Bishop M, Knight R, Belay G, Will R, Mitrova E. EUROCJD. Genetic prion disease: the EUROCJD experience. Human Genet. 2005; 118:166–174. [PubMed: 16187142]
8. Gambetti P, Kong Q, Zou W, Parchi P, Chen SG. Sporadic and familial CJD: classification and characterization. Br Med Bull. 2003; 66:213–239. [PubMed: 14522861]
9. Brown P, Brandel JP, Sato T, Nakamura Y, MacKenzie J, Will RG, Ladogana A, Pocchiari M, Leschek EW, Schonberger LB. Iatrogenic Creutzfeldt-Jakob disease, final assessment. Emerg Infect Dis. 2012; 18:901–907. [PubMed: 22607808]
10. Geschwind MD, Shu H, Haman A, Sejvar JJ, Miller BL. Rapidly progressive dementia. Ann Neurol. 2008; 64:97–108. [PubMed: 18668637]
11. Vitali P, Maccagnano E, Caverzasi E, Henry RG, Haman A, Torres-Chae C, Johnson DY, Miller BL, Geschwind MD. Diffusion-weighted MRI hyperintensity patterns differentiate CJD from other rapid dementias. Neurology. 2011; 76:1711–1719. [PubMed: 21471469]
12. Steinhoff BJ, Zerr I, Glatting M, Schulz-Schaeffer W, Poser S, Kretzschmar HA. Diagnostic value of periodic complexes in Creutzfeldt-Jakob disease. Ann Neurol. 2004; 56:702–708. [PubMed: 15449324]
13. Sanchez-Juan P, Sánchez-Valle R, Green A, Ladogana A, Cuadrado-Corrales N, Mitrová E, Stoeck K, Sklaviadis T, Kulczycki J, Hess K, Krasnianski A, Equestre M, Slivarichová D, Saiz A, Calero M, Pocchiari M, Knight R, van Duijn CM, Zerr I. Influence of timing on CSF tests value for Creutzfeldt-Jakob disease diagnosis. J Neurol. 2007; 254:901–906. [PubMed: 17385081]
14. Huang N, Marie SK, Livramento JA, Chammas R, Nitrini R. 14-3-3 protein in the CSF of patients with rapidly progressive dementia. Neurology. 2003; 61:354–357. [PubMed: 12913197]
15. Hamlin C, Puoti G, Berri S, Sting E, Harris C, Cohen M, Spear C, Bizzi A, Debanne SM, Rowland DY. A comparison of tau and 14-3-3 protein in the diagnosis of Creutzfeldt-Jakob disease. Neurology. 2012; 79:547–552. [PubMed: 22843257]
16. Atarashi R, Satoh K, Sano K, Fuse T, Yamaguchi N, Ishibashi D, Matsubara T, Nakagaki T, Yamanaka H, Shirabe S, Yamada M, Mizusawa H, Kitamoto T, Klug G, McGlade A, Collins SJ, Nishida N. Ultrasensitive human prion detection in cerebrospinal fluid by real-time quaking-induced conversion. Nat Med. 2011; 17:175–178. [PubMed: 21278748]
17. Henkel K, Zerr I, Hertel A, Gratz KF, Schroter A, Tschampa HJ, Bihl H, Bull U, Grunwald F, Drzezga A, Spitz J, Poser S. Positron emission tomography with [(18)F]FDG in the diagnosis of Creutzfeldt-Jakob disease (CJD). J Neurol. 2002; 249:699–705. [PubMed: 12111302]
18. Engler H, Lundberg PO, Ekbom K, Nennesmo I, Nilsson A, Bergström M, Tsukada H, Hartvig P, Långström B. Multitracer study with positron emission tomography in Creutzfeldt-Jakob disease. Eur J Nucl Med Mol Imaging. 2003; 30:85–95. [PubMed: 12483414]
19. Kim EJ, Cho SS, Jeong BH, Kim YS, Seo SW, Na DL, Geschwind MD, Jeong Y. Glucose metabolism in sporadic Creutzfeldt-Jakob disease: a statistical parametric mapping analysis of [18] F-FDG-PET. Eur J Neurol. 2012; 19(3):488–493. [PubMed: 22050286]
20. Engler H, Nennesmo I, Kumlien E, Gambini JP, Lundberg P, Savitcheva I, Långström B. Imaging astrocytosis with PET in Creutzfeldt-Jakob disease: a case report with histopathological findings. Int J Clin Exp Med. 2012; 5(2):201–207. [PubMed: 22567182]
21. McGeer PL, Kamo H, Harrop R, McGeer EG, Martin WR, Pate BD, Li DK. Comparison of PET, MRI, and CT with pathology in a proven case of Alzheimer's disease. Neurology. 1986; 36:1569–1574. [PubMed: 3491344]
22. Higuchi M, Tashiro M, Arai H, Okamura N, Hara S, Higuchi S, Itoh M, Shin RW, Trojanowski JQ, Sasaki H. Glucose hypometabolism and neuropathological correlates in brains of dementia with Lewy bodies. Exp Neurol. 2000; 162:247–256. [PubMed: 10739631]
23. Zhang L, Guo Y, Hu H, Wang J, Liu Z, Gao F. FDG-PET and NeuN-GFAP immunohistochemistry of hippocampus at different phases of the pilocarpine model of temporal lobe epilepsy. Int J Med Sci. 2015; 12:288–294. [PubMed: 25798055]

24. Pagani M, Chiò A, Valentini MC, Öberg J, Nobili F, Calvo A, Moglia C, Bertuzzo D, Morbelli S, De Carli F, Fania P, Cistaro A. Functional pattern of brain FDG-PET in amyotrophic lateral sclerosis. Neurology. 2014; 83:1067–1074. [PubMed: 25122207]
25. Schroeter M, Dennin MA, Walberer M, Backes H, Neumaier B, Fink GR, Graf R. Neuroinflammation extends brain tissue at risk to vital peri-infarct tissue: a double tracer [^{11}C]PK11195- and [^{18}F]FDG-PET study. J Cereb Blood Flow Metab. 2009; 29:1216–1225. [PubMed: 19352400]
26. Puoti G, Giaccone G, Mangieri M, Limido L, Fociani P, Zerbi P, Suardi S, Rossi G, Iussich S, Capobianco R, Di Fede G, Marcon G, Cotrufo R, Filippini G, Bugiani O, Tagliavini F. Sporadic Creutzfeldt-Jakob disease: the extent of microglia activation is dependent on the biochemical type of PrPSc. J Neuropathol Exp Neurol. 2005; 64:902–909. [PubMed: 16215462]
27. Szpak GM, Lewandowska E, Lechowicz W, Wierzba-Bobrowicz T, Kulczycki J, Bertrand E, Pasennik E, Dymecki J. The brain immune response in human prion diseases. Microglial activation and microglial disease. I. Sporadic Creutzfeldt-Jakob disease. Folia Neuropathol. 2006; 44:202–213. [PubMed: 17039416]
28. Wojtera M, Sobow T, Kloszewska I, Liberski PP, Brown DR, Sikorska B. Expression of immunohistochemical markers on microglia in Creutzfeldt-Jakob disease and Alzheimer's disease: morphometric study and review of the literature. Folia Neuropathol. 2012; 50:74–84. [PubMed: 22505366]
29. Llorens F, López-González I, Thüne K, Carmona M, Zafar S, Andréoletti O, Zerr I, Ferrer I. Subtype and regional-specific neuroinflammation in sporadic Creutzfeldt-Jakob disease. Front Aging Neurosci. 2014; 6:198. eCollection 2014. [PubMed: 25136317]
30. Baumgartner A, Rauer S, Mader I, Meyer PT. Cerebral FDG-PET and MRI findings in autoimmune limbic encephalitis: correlation with autoantibody types. J Neurol. 2013; 260:2744–2753. [PubMed: 23900756]
31. Sobrado M, Delgado M, Fernández-Valle E, García-García L, Torres M, Sánchez-Prieto J, Vivancos J, Manzanares R, Moro MA, Pozo MA, Lizasoain I. Longitudinal studies of ischemic penumbra by using ^{18}F-FDG PET and MRI techniques in permanent and transient focal cerebral ischemia in rats. Neuroimage. 2011; 57:45–54. [PubMed: 21549205]

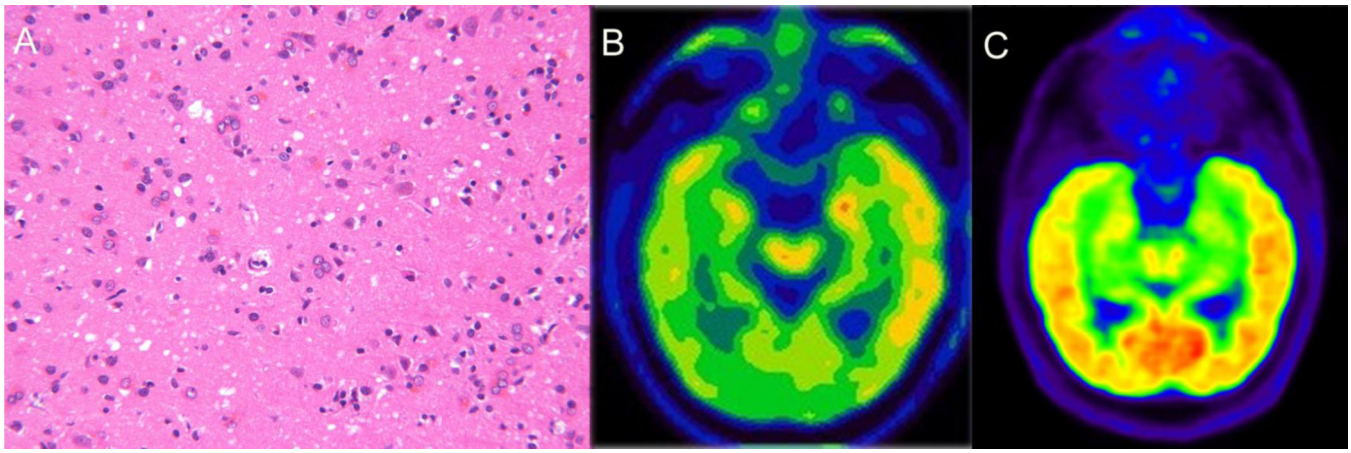

Figure 1. Neuropathology and FDG-PET in CJD

A. Moderate neuronal loss, reactive astrocytosis and spongiosis on hematoxylin and eosin staining in the occipital cortex in a case of MM1 subtype of CJD (Case #11). B. FDG-PET hypometabolism in temporal, parietal, and occipital lobes and hypermetabolism in the left medial temporal region in a case of MM1 subtype of CJD (Case #11). C. Normal FDG-PET shown for comparison.

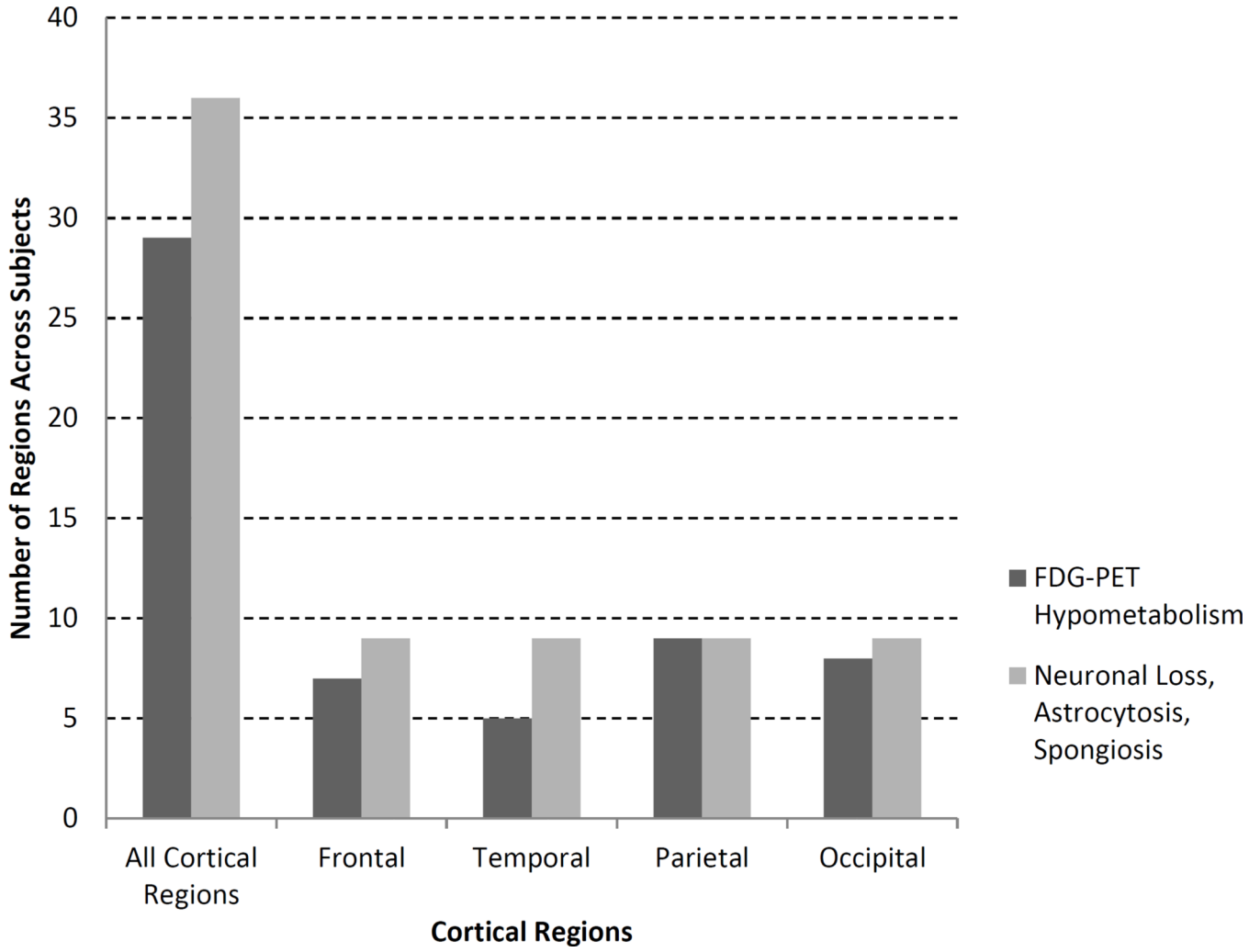

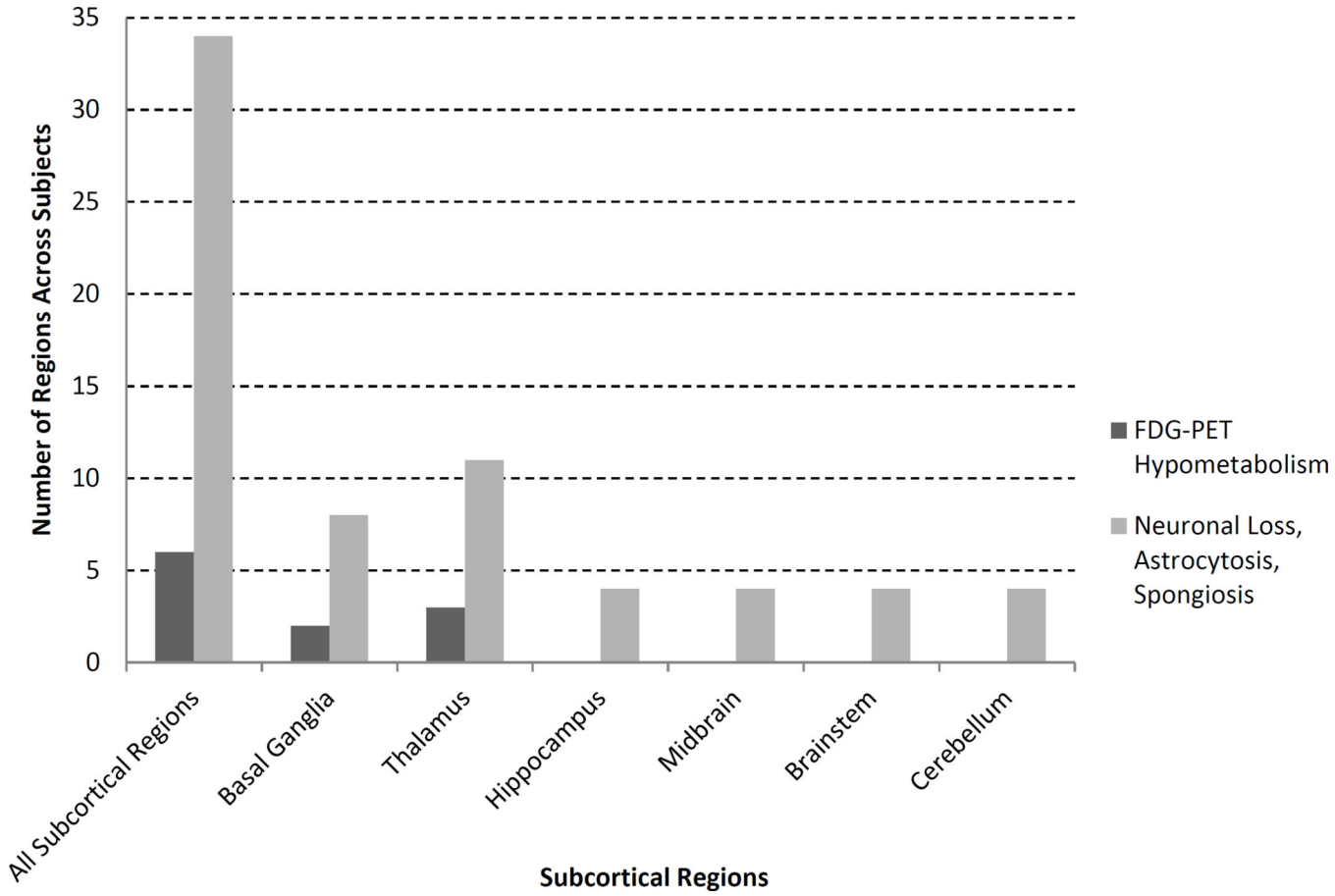

Figure 2. Regional FDG-PET Hypometabolism and Neuropathology

A. Cortical Regions. This chart shows number of cortical regions with neuronal loss, astrocytosis and/or spongiosis that showed hypometabolism on FDG-PET for all cases of definite prion disease together. B. Subcortical Regions. This chart displays subcortical regions with neuronal loss, astrocytosis, and/or spongiosis that showed hypometabolism on FDG-PET.

Table 1

Patient Characteristics

Patient #	Age (yrs)	Sex	Survival Time (months)	Onset to PET scan (months)	PET to Death (months)	Classification	Clinical Presentation	CSF 14-3-3	CSF Tau (pg/mL)[a]	EEG	MRI DWI Hyperintensities	Molecular Subtype or Genotype
1	39	M	4	2	2	Definite (FFI)	Dementia, insomnia, myoclonus, pyramidal	Negative	456	Slowing	None	D178N-129M
2	62	F	26	12	14	Definite (sCJD)	Dementia, behavior	Ambiguous	562	Slowing	Cortical	MV2
3	79	M	2	1	1	Definite (sCJD)	Dementia, ataxia, myoclonus, pyramidal, visual	Positive	11892	PSWCs	Cortical, caudate	MM1
4	66	M	10	3	7	Definite (sCJD)	Dementia, visual	Ambiguous	874	No PSWCs	cortical	MV2
5	42	F	32	8	24	Definite (sCJD)	Dementia, ataxia, behavior, extrapyramidal, myoclonus	Ambiguous	1310	Slowing	cortical	MM2
6	56	F	12	8	4	Definite (sCJD)	Dementia, extrapyramidal, myoclonus	Not available	Not available	Normal	Cortical, caudate	MM2
7	46	M	2	2	0.25	Definite (gCJD)	Dementia, behavior, insomnia myoclonus, pyramidal	Ambiguous	723	Slowing	None	E200K-129M
8	66	F	5	2	3	Definite (gCJD)	Dementia, extrapyramidal, pyramidal	Ambiguous	3886	PSWCs	Cortical, caudate	E200K-129M
9	59	F	7.5	6	1.5	Definite (sCJD)	Dementia, ataxia, myoclonus	Positive	8029	Slowing	Caudate	VV2
10	57	M	12	10.5	1.5	Definite (sCJD)	Dementia, ataxia, myoclonus	Positive	8975	slowing	Caudate	VV2
11	72	F	6	5	1	Definite (sCJD)	Dementia, extrapyramidal, pyramidal, visual	Positive	5175	PSWCs	Cortical, caudate	MM1

[a] CSF tau is defined as positive if greater than 1150 pg/mL (Hamlin et al., 2012)

gCJD, genetic CJD; PSWCs, periodic sharp wave complexes; sCJD, sporadic CJD

Table 2

Hypometabolic and Hypermetabolic Regions

Hypometabolic Regions	Number of Cases
Precuneus	11 (100%)
Posterior Cingulate Gyrus	10 (90.9%)
Cuneus	8 (72.7%)
Hypermetabolic Regions	**Number of Cases**
Insula	11 (100%)
Medial Temporal Lobe	10 (90.9%)
Nucleus Accumbens	10 (90.9%)
Olfactory Cortex	10 (90.9%)
Parahippocampal Gyrus	10 (90.9%)
Amygdala	9 (81.8%)
Hippocampus	9 (81.8%)

Table 3

Percentage of Regions with FDG-PET Hypometabolism and Neuronal Loss/Astrocytosis/Spongiosis

Region	Percentage of Neuronal Loss/Astrocytosis/Spongiosis with FDG-PET Hypometabolism
Cortical Regions	80.6%
Frontal	77.8%
Temporal	55.6%
Parietal	100%
Occipital	88.9%
Subcortical Regions	17.6%
Basal Ganglia	25%
Thalamus	27.3%
Hippocampus	0%
Midbrain	0%
Brainstem	0%
Cerebellum	0%